Earthquake Response Analysis of Elastoplastic Structure-Ground Systems of Shear Type by the Direct Numerical Analysis Method

by Yoshihisa GYŌTEN(I), Kōji MIZUHATA(II), Yūichi FUKUDA(III)
Michiaki KAWAMOTO(III), Tadaaki SHINOMIYA(III)

Synopsis

In this study, a structure-ground system is idealized to be a shear beam on the ground of shear type and the direct numerical analysis method is applied to its elastoplastic earthquake response analysis and the analysis of earthquake waves on the bed rock. This method is based on direct use of the governing physical laws and initial and boundary conditions and bypasses the wave equation. Elastoplastic earthquake responses and earthquake waves on the bed rock are plotted by taking the area ratio and the impedance ratio of the building and the ground as parameters.

Introduction

Usually, in the earthquake response analysis of a building-ground system, both the structure and the ground are idealized to be lumped mass-spring systems and for this model the equations of motion are derived and solved numerically by the Runge-Kutta's method, etc.. In this method, however, it is difficult to make a lumped mass-spring system model of the ground. On the other hand, the structure as well as ground are idealized often to be elastic continuous bodies and the wave equation for this model is derived and solved numerically. This method enables one to obtain the standing or the traveling wave solution and to know process of wave propagation including reflection and transmission, but there are difficulties in taking into account variations of cross section and plasticity for obtaining the response due to random excitation such as earthquake motion. In the case that the ground is considered to be elastoplastic, the finite element method is adopted, but this does not give the rigorous solution and enormous amount of memory and time are needed in digital computation. Then in this study, the direct numerical analysis method, which was partially developed in the analyses of the spherical waves and of impact of cylinders on rigid targets(I), has been applied to the elastoplastic earthquake response analysis of the structure-ground system and its behavior during earthquake has been investigated. By the way, by this method earthquake waves on the bed rock have also been obtained under the consideration of the structure and the ground. In the direct numerical analysis method, the differential equation is bypassed, and the governing physical laws and kinematical relations are used directly to the model under consideration which is previously divided into a finite number of cells. Such physical laws are (1) Characteristic assumption, (2) Relation between strain and displacement, (3) Material constitutive equation, and (4) Impulsive momentum law. This method gives the rigorous solution and also this is the most suitable for use of automatic digital computers, because successive operations of the physical laws expressed in difference form are the computer instructions, themselves. Even for large number of cells, comparatively small memory and short time are enough in the computer.

Basic Procedure of the Direct Numerical Analysis Method

A structure-ground system is idealized to be the shear beam as shown

(I),(II),(III): Prof., Assoc. Prof., Former Grad. Stud. at Kobe Univ., Kobe

in Fig.1. The x-axis is taken in the axial direction and the y-axis in the lateral direction. This shear beam consists of the material with the bilinear constitutive relationship $\tau=G_e\gamma_y+G_p(\gamma-\gamma_y)$ ····· (1)
as shown in Fig.2, where τ,γ: shear stress and strain, γ_y: yield shear strain, G_e,G_p: elastic and plastic shear constants. The elastic and the plastic waves propagate by the velocities of $C_e=\sqrt{G_e/\rho}$, $C_p=\sqrt{G_p/\rho}$ ····· (2)
respectively. When the shear beam is divided into a finite number i_n of cells along its height, length of each cell, dx_i, is given by
$dx_i=C_e dt_e$ for elastic region and $dx_i=C_p dt_p$ for plastic region ····· (3)
which is called the characteristic assumption, where dt_e, dt_p are the time increments in the elastic and the plastic regions, respectively. dx_i or dt should be chosen to keep the stability of calculation in relation to the frequency characteristics of the external disturbance and the structure. The impulsive momentum law is written as $m_i\times dv_i=dQ_i\times dt$ ····· (4)
where m_i is the mass of the i-th element and dv_i is the incremental particle velocity due to the net force dQ_i applied to the cell during the incremental time dt. Since $m_i=\rho_i A_i dx_i$ and $dQ_i=A_i d\tau_i$, where A_i, ρ_i, and $d\tau_i$ are the cross-sectional area, density of the i-th cell and the incremental shear stress, respectively, then $dv_i=d\tau_i/\rho_i C$ ····· (5)
or $d\tau_i=\rho_i C_e dv_i$ for elastic wave and $d\tau_i=\rho_i C_p dv_i$ for plastic wave ···· (6)
The cummulation condition for velocity is stated as $v_i\leftarrow v_i+dv_i$ ····· (7)
and that for stress is as $\tau_i\leftarrow\tau_i+d\tau_i$ ····· (8)
by introducing a replacement symbol of the computer. The incremental displacement dy_i can be obtained $dy_i=v_i dt$ and the shear strain γ_i can be obtained by the strain-displacement relation $\gamma_i=dy_i/dx_i$. The displacement is cummulated as $y_i\leftarrow y_i+dy_i$ ····· (9)
For the downward going waves, procedure is the same as for the upward going wave except $d\tau_i=-\rho_i C_i dU_i$, where dU_i denotes the incremental particle velocity of the downward going wave. Dynamic responses can be obtained by directing the operations of relations (1)∿(9) repetitively from i=0 to $i=i_n$ and repeating successively for a specified number t_e of time intervals under given initial and boundary conditions and the conditions of wave interaction. The general flow-chart is shown in Fig.3, where v is written as V.

Earthquake Response of Elastoplastic Structure-Ground Systems

(1) Interaction of Waves: When more than two waves encounter on x=i at t=t, the state after the wave interaction is determined by the yield condition and the condition of continuity of the shear stress and the particle velocity. In the following, the fully-elastoplastic case is explained, though Figs.4(a)∿(i) show the cases where the plastic wave velocity is finite. In general, nine cases as shown in Figs.4(a)∿(i) are possible, but Figs.4(c),(e), and (f) are proved to be the same by calculations. Also, Figs.4(a)∿(f) can be expressed by the same equations. The flow-chart of wave interaction in Fig.4 is shown in Fig.5. As an example, the wave interaction is explained in detail for the case where the forward going plastic wave and the backward going elastic wave come across and the state after interaction is elastic as shown in Fig.6(a). The conditions of continuity are

$$\left.\begin{aligned} V-\Delta V_p+\Delta U_e+\Delta V'=V\mp\Delta U' \\ \tau-\rho C_p\cdot\Delta V_p-\rho C_e\cdot\Delta U_e+\rho C_e\cdot\Delta V'=\tau-\rho C_e\cdot\Delta U' \end{aligned}\right\} \quad \cdots\cdots (10)$$

where V and V' are the particle velocities and τ and τ' are the shear stresses before and after interaction, respectively. ΔV and ΔU denote the increments of the forward and the downward going waves, respectively, the suffixes, e and p, stand for the elastic and the plastic waves, respectively

and the single prime ' means "after interaction". For the fully-plastic material, $\rho C_p \cdot \Delta V_p$ vanishes, because $C_p=0$. From Eqs.(10), $\Delta V'_e$ and $\Delta U'_e$ is solved as follows: $\Delta V'_e=\Delta V_p/2$ and $\Delta U'_e=\Delta U_e-\Delta V_p/2$ ·····(11)
Then, the new shear stress τ'_i becomes as $\tau'_i=\tau_i+\rho C_e(\Delta V'_e-\Delta U_e)$ ····· (12)
If the yield condition $|\tau'_i|\leq\tau_y$ or $-\tau_y\leq\tau_i+\rho C_e(\Delta V'_e-\Delta U_e)\leq\tau_y$ ····· (13)
is not satisfied, it is known that the plastic wave does not vanish and the state appears as Fig.6(b), where $\Delta V'_e=\Delta U_e$, $\Delta V'_p=\Delta V_p-2\Delta U_e$, $V'=V$, $\tau'=\tau$.

(2) Boundary Conditions: On the fixed end, the stress waves are reflected in phase, and seven cases as shown in Figs.7(a)∿(f) are possible. On the free end, the velocity waves are reflected in phase and the plastic wave is not generated. On the structure-ground boundary, the interaction phenomena are divided into the following three major types: (i) $AR\cdot\tau_{sy}<\tau_{Gy}$: structure yield type, (ii) $AR\cdot\tau_{sy}=\tau_{Gy}$: both yield type, and (iii) $AR\cdot\tau_{sy}>\tau_{Gy}$: ground yield type, where $AR=A_s/A_G$. Since $A\rho C$ varies on the boundary, the boundary conditions are identical to the wave interaction including transmission and reflection of waves. For the type (i) six cases as shown in Figs.8(a)∿(f), for the type (ii) seven cases in Figs.9(a)∿(g), and for the type (iii) six cases in Figs.10(a)∿(f) are possible.

(3) Numerical Results and Discussions: In the numerical analysis, the dynamic responses of the following models were calculated:
(a) A uniform shear beam of 32 cells with the restoring force characteristics of bilinear type in which $G_e/G_p=4$ and $\tau_y=80$ is subjected to the rectangular velocity disturbances of $6\Delta t_p$ long whose maximum value is twice as much as $\tau_y/\rho C_e$ as shown in Fig.11. This simple model was chosen to show clearly the elastoplastic wave propagation phenomena. The x-t computer output of the shear stress results is shown in Fig.11, where the wave fronts are shown by the solid border lines between different values. At A, both the elastic wave AG and the plastic wave AC are generated due to the instantaneous disturbance bigger than the yield stress, and at B, the unloading elastic wave BC is generated due to removal of the disturbance. This faster unloading wave BC reaches the slower plastic wave AC at C and both upward and downward going elastic waves are generated by the effect of wave interaction. At D, the upward going elastic wave CD encounters the downward going elastic wave reflected at the free top end G and two elastic and two plastic waves are generated. The plastic wave can be also generated, like as at E, when the elastic wave passes through the cells whose hystereses differ from each other, even though more than two waves do not encounter.
(b) A structure of 45m tall on the ground of 15m deep is subjected to the El Centro EW type earthquake. Both the structure and the ground are the uniform shear beams with the fully-elastoplastic restoring force characteristics. In the structure, the floor weight of 1.2ton/m^2 is distributed uniformly along its story height of 3m, mass density being 0.408×10^{-3}gr·sec^2/cm^4. The elastic shear wave velocity of the structure C_s is obtained from the fundamental natural period T_s or the number of story N and the height H_s as $C_s=4H_s/T_s=4H_s/0.08N=150$m/sec, though C_s can be calculated by the relation (2). For this value of C_s, $G_s=\rho_s C_s=0.918\times10^5$gr/cm^2. The yield shear stress of the structure $\tau_{sy}=400$gr/cm^2 is considered. For this value of τ_{sy}, the yield shear strain γ_{sy} and the yield base shear coefficient C_B become as $\gamma_{sy}=\tau_{sy}/G_s=1/230$ and $C_B=\tau_{sy}/\rho_s H_s=0.222$. Mass density of the ground ρ_G is 0.204×10^{-2}gr·sec^2/cm^4 corresponding to 2ton/m^3 and two

elastic shear wave velocities were chosen as C_G=100m/sec slower than Cs and C_G=250m/sec faster than C_s. For these values of C_G, the natural period T_G and the shear rigidity G_G are obtained as $T_G=4H_G/C_G$=0.60sec and G_G= 0.204×10^6gr/cm^2 for C_G=100m/sec, and T_G=0.24sec and $G_G=0.128\times10^7$gr/cm^{2}for C_G=250m/sec. Although there are many discussions on the hysteresis loops of the ground in other papers, in this study as the first step of the elastoplastic analysis, the hysteresis loop of the ground is assumed to be of fully-elastoplastic type whose yield stress τ_{Gy} and strain γ_{Gy} are 1000gr/cm^2 and 7.85×10^{-4} respectively for the stiffer ground and 400gr/cm^2 and 19.6×10^{-4} respectively for the softer ground by the inspection of existing soil test data. The effective cross-sectional area of the ground A_G varies from the area of the structure A_s to that of the ground A_G. Four area ratios of the ground and the structure $D=A_G/A_s$ of 1,3,5, and 10 are considered for the purpose of the parametric survey covering the range near the observed value of 3[2]. As the external disturbance on the bed rock, the El Centro EW type earthquake of 9sec long is applied. Its maximum amplitude was chosen to be 1gal for the elastic system, while for the elastoplastic system, to be 113gal, the minimum acceleration making the structure with the fixed base yield, and 170gal, one and a half times as much as 113gal. The maximum responses of the floor displacement and the shear stress or the ductility factor along height have been plotted for the elastoplastic structure with the fixed base in Figs.12(a) and (b), for the elastic structure-ground system (whole elastic system) in Figs.13(a)∿(d), for the elastoplastic structure-elastic ground system (partially elastoplastic system) in Figs.14(a)∿(h), and for the elastoplastic structure-ground system (whole elastoplastic system) in Figs.15(a)∿(h). From the reponse diagrams in Figs. 12∿15, the followings are stated. As the area ratio $D=A_G/A_s$ increases, the displacement response of the upper part of the structure becomes larger for the whole elastic system, but it does not always for the partially and whole elastoplastic systems. This is because, as shown in Figs.14(b),(d), (f), and (h), the structure yields in the middle and the lower parts, where the energy is consumed. This tendency is exaggerated and the distribution along height becomes more complicated, as the maximum acceleration of the disturbance relative to the structure increases. It should be kept in mind that intensity of the disturbance relative to the structure is enlarged as the area ratio increases because of the stress concentration on the structure-ground boundary. From this point of view, it recognized that D=10 in this one-dimensional model may not be appropriate. In the responses of the whole elastic system, the second (for the softer ground) or the third (for the harder ground) modes can be observed clearly because of the psudo-resonance to the predominant period of the ground or the disturbance, while in the responses of both elastoplastic system, this tendency becomes smaller. The whole elastoplastic system with the softer ground yields greatly on the bottom of the ground and on the structure-ground boundary. Therefore, the ductility factor in the structure which was large in the middle part in the partially elastoplastic analysis, becomes smaller and smoother as shown in Fig.15(b) and resembles the elastoplastic response of the structure on the fixed base where the ductility factor is large also on the bottom in Fig.12 (b). The ductility factor is larger on the bottom of the ground than on the structure-ground boundary for the softer ground, while for the harder ground, the result is reverse. Although the structure-ground system models analyzed have the specific dimensions, such as the structure of 45m tall and the ground of 15m deep, it can be considered from the view-point of

rigidity and strength ratios that the combination of the structure with C_s =150m/sec and the ground with C_G=100m/sec corresponds to a short rigid structure on a softer ground and that the combination of the structure with C_s=150m/sec and the ground with C_G=250m/sec corresponds to a tall flexible structure on a harder ground. Therefore, the results in this study can be applied to these situations. The x-t computer outputs for the elastoplastic structure-ground systems of D=5 subjected to the El Centro EW type earthquake of 170gal are shown in Figs.16(a) and (b), where the symbol 0 denotes the elastic region and the symbols, + and -, denote the plastic region. Fig.16(a) is for the case of C_G=100m/sec and (b) is for C_G=250m/sec. It is mentioned from Fig.16 that in the case of C_G=100m/sec less number of larger plastic regions appear, while in the case of C_G= 250m/sec more number of smaller plastic regions scatter. It is seen that the elastic-plastic boundary is along four characteristic lines.

Earthquake Waves on the Bed Rock

The problem taken up here as another application of the direct numerical analysis method is to calculate the earthquake waves considered to have entered from the bed rock in terms of the earthquake wave recorded on the base of the structure by taking into account the characteristics of both the structure and the ground. In Fig.17(a), VB_1, VB_2,..., VB_n,... are considered to be the time series of the particle velocity of an earthquake recorded on the base of the structure on the ground, where both are idealized to be one-dimensional elastic continuous bodies of shear type as shown in Fig.1. The wave interaction on the structure-ground interface at the beginning is shown in Fig.17(a). In Fig.17(b), the wave interaction when the wave reflected at the free top end reaches the interface is shown. In Fig.17(c), the reflection of waves on the fixed bed rock end is shown. The time series of the particle velocity of the earthquake waves on the bed rock VG_1, VG_2,..., VG_n,... can be obtained by following the flow-chart drawn in Fig.18, where a and b denote the reflection and the transmission coefficients, respectively, and $R=A_s\rho_s C_s/A_G\rho_G C_G$. In the numerical analysis four combinations of two structures with different fundamental natural periods of 0.80sec and 0.64sec and two grounds with different predominant periods of 0.96sec and 0.72sec were considered as shown in the left side of Fig.20. The natural period of the structure is taken to be the periods corresponding to the inverted peaks in the power spectrum of the external disturbance and the predominant period of the ground is taken to be the periods corresponding to the peaks in the same spectrum. Four area ratios of the structure and the grounds A_G/A_s=1,3,5, and ∞ are considered for the purpose of the parametric survey covering the range near the observed value of 3[2]. The area ratio of ∞ corresponds to the model of the ground, only. As an example of the earthquake wave recorded on the base of the structure, the particle velocity wave of El Centro NS earthquake of 1gal as shown in Fig.19 integrated by the Simpson's Formula, is adoped. Figs.20(a)∿(d) show the earthquake waves on the bed rock for the cases 1∿4, respectively, with time by taking the area ratio as parameter. Figs.21(a)∿(c) show the earthquake waves on the bed rock with time for the area ratio D=1,5, and ∞ to compare the effect of the natural periods of the structure and the ground. The followings are mentioned from Figs.20 and 21: The earthquake wave on the bed rock for the case 1 resembles that for the case 3 and that for the case 2 resembles that for the case 4. Except the early stage the natural periods of the structure 0.80sec and 0.64sec which were not observed in the

earthquake record on the base, are predominant, while the predominant periods of the ground disappear, that is, both the peaks and the inverted peaks in the spectrum of the earthquake record disappear. This result coincides with the theoretical one. This fact shows the validity of this method, also. The earthquake waves on the bed rock for the area ratio D=3 and those for D=5 are very similar each other, while that for D=1 is different from others. For D=1, difference due to the cases is large, that is, the effect of the structure is large. As the area ratio increases, the effect of the structure decreases and finally disappears for D=∞, which corresponds to the case that the structure is removed. The true earthquake wave on the bed rock may be calculated by this method from the wave recorded on the base of the structure by considering the true characteristics of the structure and the ground at El Centro.

Conclusions

The elastoplastic earthquake responses of the shear beam type structure-ground system were successfully obtained by the direct numerical analysis method which is based on the direct use of the physical laws and initial and boundary conditions. As the area ratio A_G/A_s increases, the displacement response of the upper part of the structure becomes larger for the elastic system, but it does not always for the elastoplastic system, because the structure yield the middle and the lower parts where the energy is consumed. The whole elastoplastic system on the softer ground yields greatly on the bottom of the ground and on the structure-ground boundary, the ductility factor in the structure becomes smaller and resembles the elastoplastic response of the structure on the fixed base where the ductility factor is large also on the bottom. The ductility factor is large on the bottom of the ground than on the structure-ground boundary for the softer ground, while for the harder ground, the results is reverse. By the way, the direct numerical analysis method is applied to calculate the earthquake wave on the bed rock from the earthquake wave recorded on the base of the structure by taking into account the characteristics of both the structure and the ground. As the results, it is mentioned that both the peaks and the inverted peaks in the spectrum of the earthquake wave recorded on the base of the structure disappear. For both problems, though the area ratio is changed parametrically, the true area ratio shall be determined by actual observations. It is reported in Ref.(2) that the area ratio of 3 was observed. The direct numerical analysis method gives the rigorous elastoplastic solution at each cell position and can give the sharp wave front. Also, this method is very suitable for use of automatic digital computer to analyze the elastoplastic wave propagation in the continuous body, because small memory and short time is enough in computers.

Bibliography

(1) Raftopoulos, D. and N. Davids, "Plastic Impact of Cylinders on Rigid Targets," Tech. Rep., Dept. of Eng. Mechs., Penn. State Univ., Dec. 15, 1965

(2) Ōsawa Y. et al., "Analysis of Earthquake Motions Recorded in a Building-Subsoil System," Proc. of the 3rd Japan Earthquake Eng. Symp., 1970

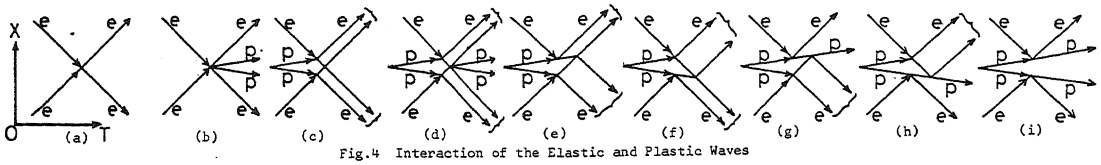

Fig.4 Interaction of the Elastic and Plastic Waves

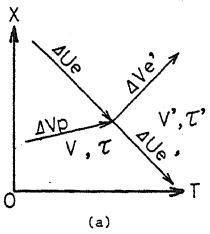

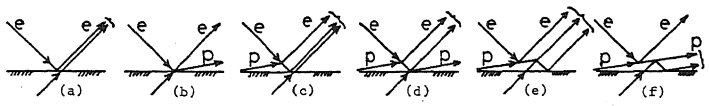

Fig.7 Wave Interaction at the Fixed End

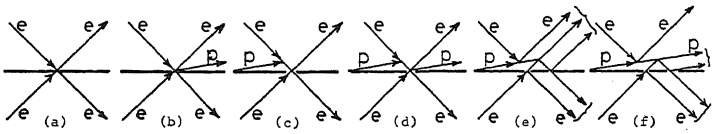

Fig.8 Wave Interaction on the Structure-Ground Boundary for the Structure Yield Type

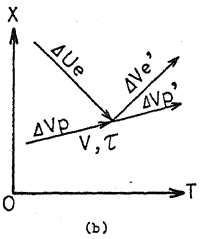

Fig.6 Wave Interaction for an Example

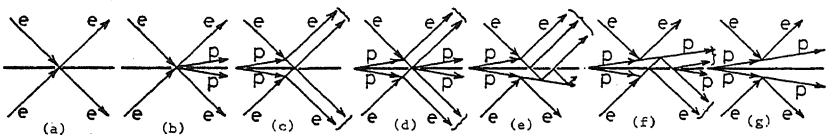

Fig.9 Wave Interaction on the Structure-Ground Boundary for the Both Yield-Type

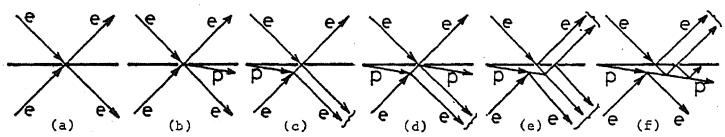

Fig.10 Wave Interaction on the Structure-Ground Boundary for the Ground Yield Type

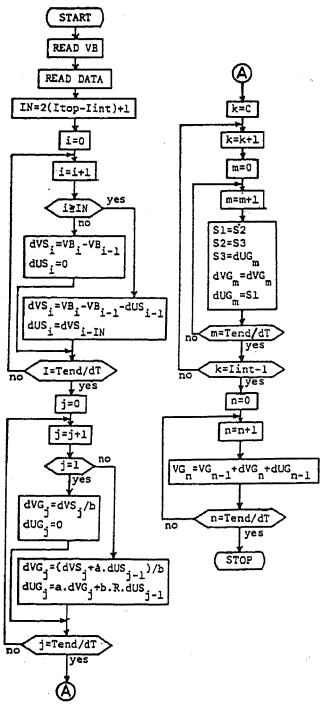

Fig.18 Flow Chart for Obtaining the Earthquake Wave on the Bed Rock

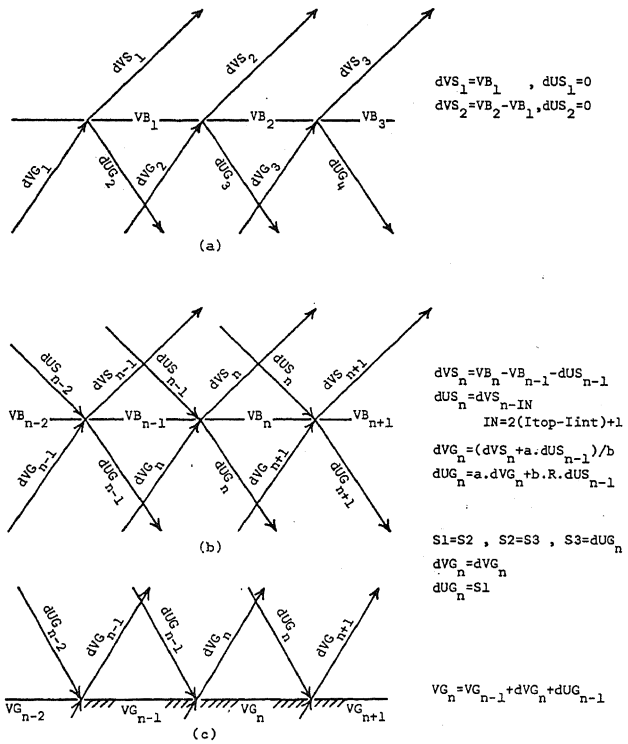

Fig.17 Wave Interaction on the Structure-Ground Interface

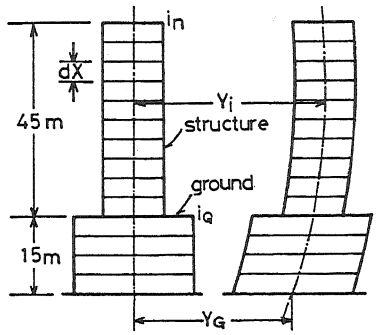

Fig.1 Structure-Ground System Model

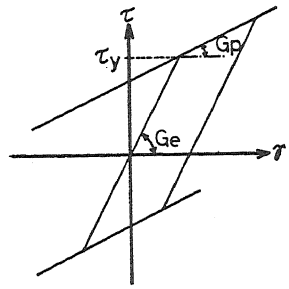

Fig.2 Elastoplastic Constitutive Relation

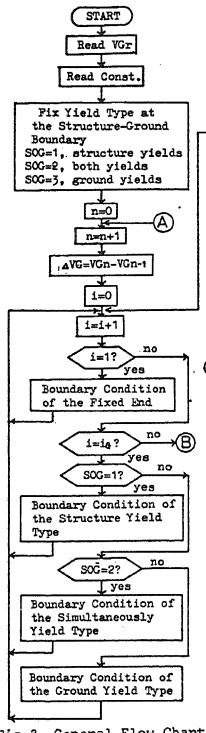

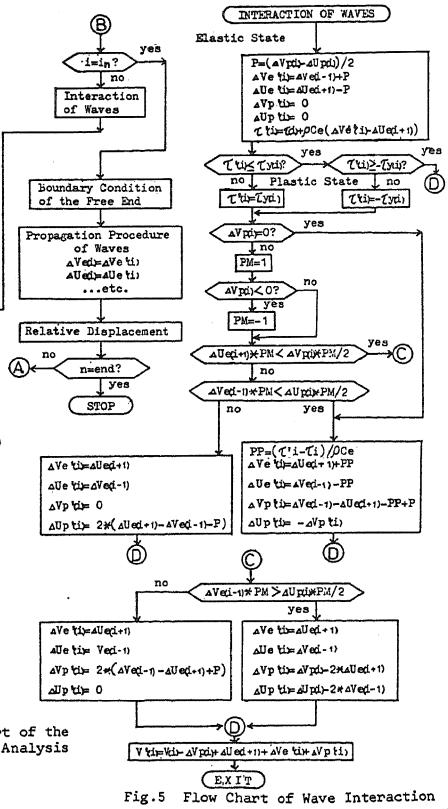

Fig.3 General Flow Chart of the Elastoplastic Response Analysis

Fig.5 Flow Chart of Wave Interaction

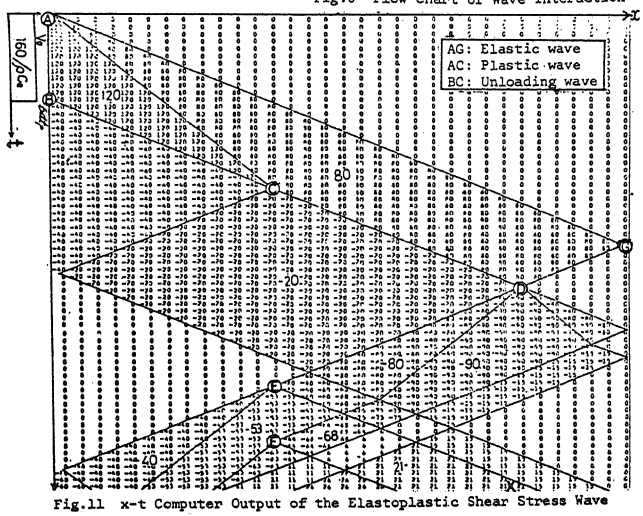

Fig.11 x-t Computer Output of the Elastoplastic Shear Stress Wave

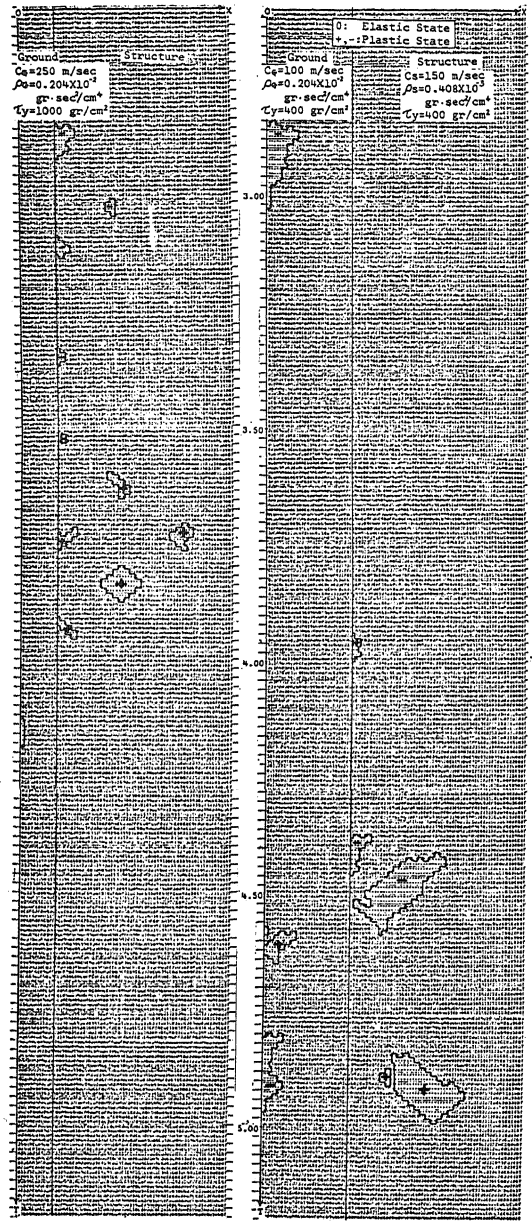

Fig.16 x-t Computer Output of the Earthquake Response of the Elastoplastic Structure-Ground System
(a) For the Harder Ground
(b) For the Softer Ground

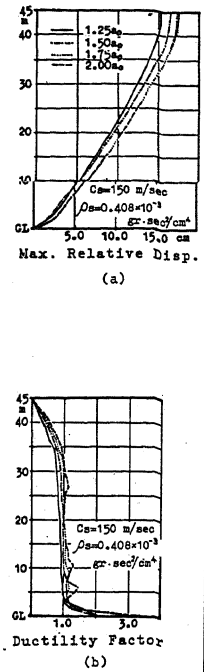

Fig.12 Elastoplastic Earthquake Response of the Structure with the Fixed Base

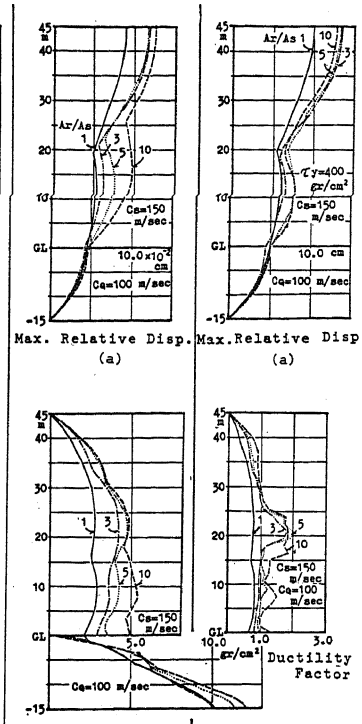

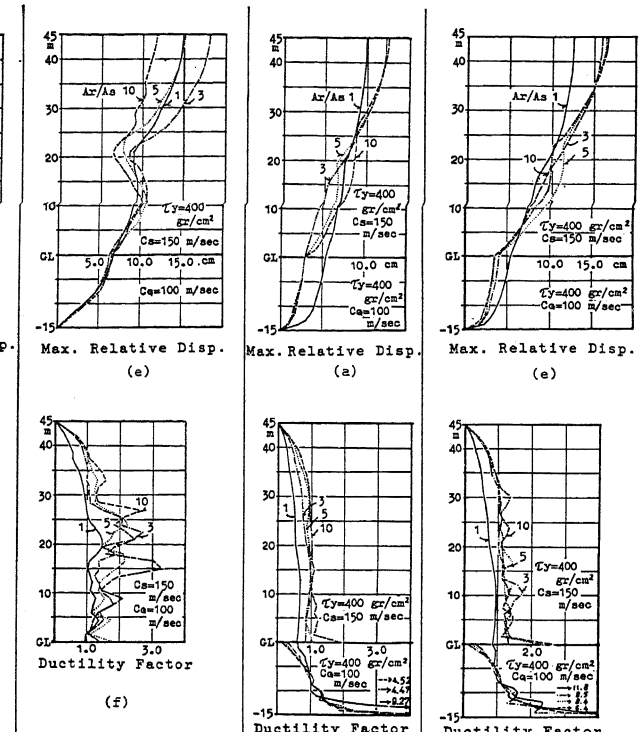

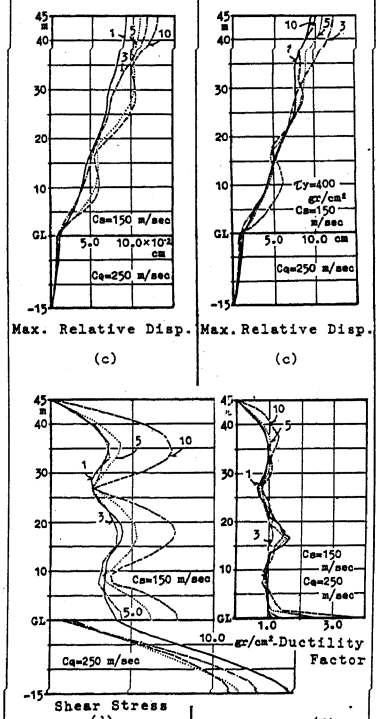

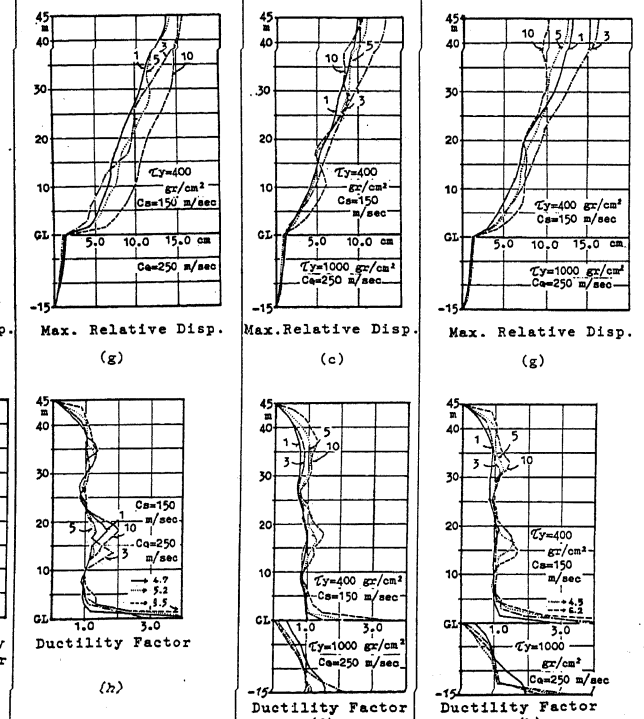

Fig.13 Earthquake Response of the whole Elastic Structure-Ground System
($\rho_s=0.408\times10^{-3}$ gr·sec²/cm⁴, $\rho_G=0.204\times10^{-2}$ gr·sec²/cm⁴, Max. Input 1 gal)

Fig.14 Earthquake Response of the Elastoplastic Structure-Elastic Ground System
($\rho_s=0.408\times10^{-3}$ gr·sec²/cm⁴, $\rho_G=0.204\times10^{-2}$ gr·sec²/cm⁴, (a)∿(d) Max. Input 113 gal, (e)∿(h) Max. Input 170 gal)

Fig.15 Earthquake Response of the Whole Elasto-plastic Structure-Ground System
($\rho_s=0.408\times10^{-3}$ gr·sec²/cm⁴, $\rho_G=0.204\times10^{-2}$ gr·sec²/cm⁴, (a)∿(d) Max. Input 113 gal, (e)∿(h) Max. Input 170 gal)

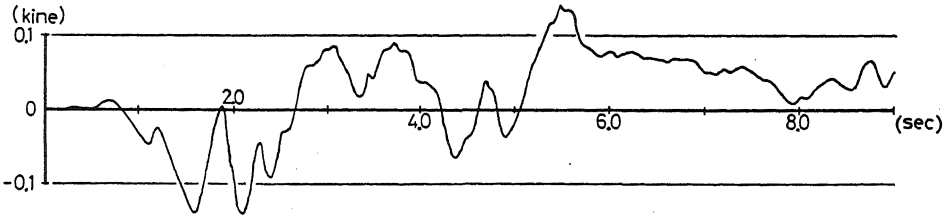

Fig.19 Particle Velocity Wave of the Earthquake Recorded on the Base of the Structure

CASE 1	T (sec)	H (m)	V (m/sec)
STRUCTURE	0.80	30.0	150.0
GROUND	0.96	60.0	250.0

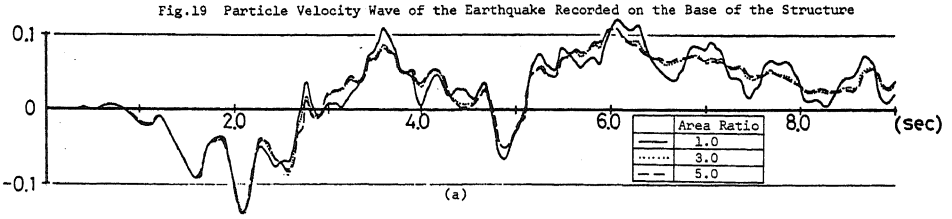

CASE 2	T (sec)	H (m)	V (m/sec)
STRUCTURE	0.64	24.0	150.0
GROUND	0.96	60.0	250.0

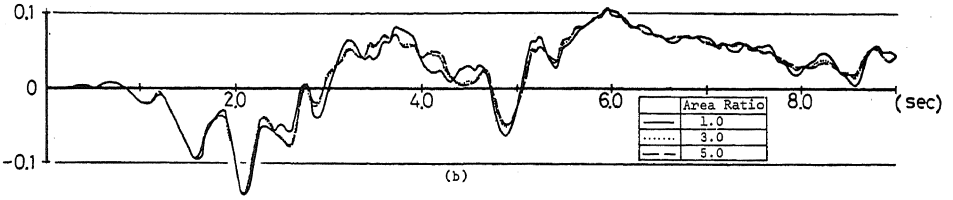

CASE 3	T (sec)	H (m)	V (m/sec)
STRUCTURE	0.80	30.0	150.0
GROUND	0.72	45.0	250.0

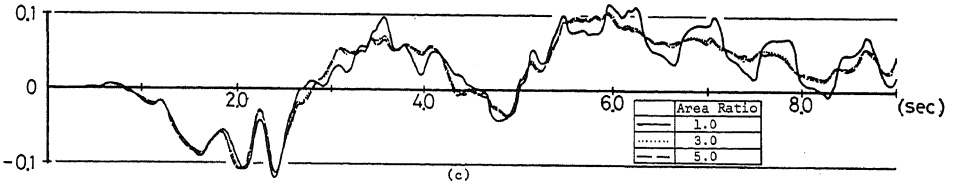

CASE 4	T (sec)	H (m)	V (m/sec)
STRUCTURE	0.64	24.0	150.0
GROUND	0.72	45.0	250.0

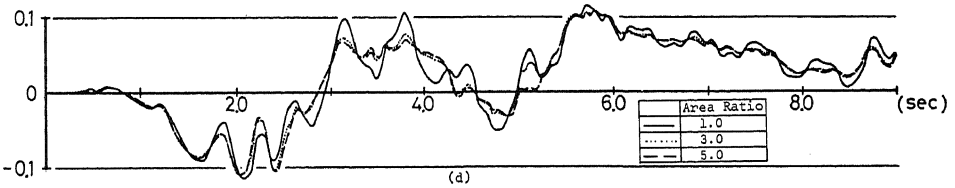

Fig.20 Earthquake Waves on the Bed Rock by Taking the Area Ratio as Parameter

AREA RATIO = 1.0

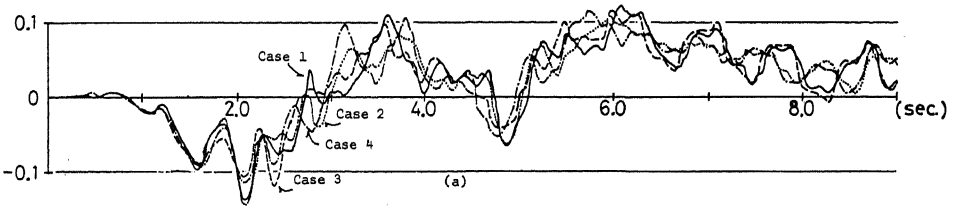

AREA RATIO = 5.0

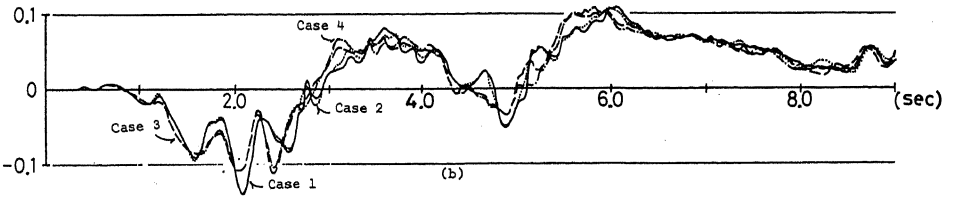

AREA RATIO = ∞

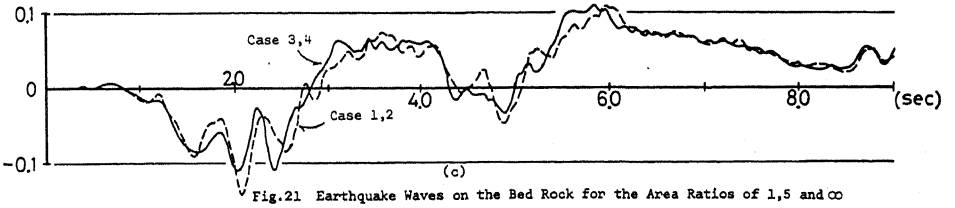

Fig.21 Earthquake Waves on the Bed Rock for the Area Ratios of 1,5 and ∞